Proceedings of the ASME 2014 33rd International Conference on Ocean, Offshore and Arctic Engineering
OMAE 2014
June 8-13, 2014, San Francisco, USA, California

OMAE2014-23152

WAVES' NUMERICAL DISPERSION AND DAMPING DUE TO DISCRETE DISPERSION RELATION

Babak Ommani
MARINTEK,
P.O.Box 4125 Valentinlyst
NO-7450 Trondheim, Norway
Phone: +47 40 33 20 32, Fax: +47 73 51 00 34
Email: babak.ommani@marintek.sintef.no

Odd M. Faltinsen
Centre for Autonomous Marine Operations and Systems (AMOS),
Department of Marine Technology, NTNU,
NO-7491 Trondheim, Norway
Email: odd.faltinsen@ntnu.no

ABSTRACT

In linear Rankine panel method, the discrete linear dispersion relation is solved on a discrete free-surface to capture the free-surface waves generated due to wave-body interactions. Discretization introduces numerical damping and dispersion, which depend on the discretization order and the chosen methods for differentiation in time and space. The numerical properties of a linear Rankine panel method, based on a direct boundary integral formulation, for capturing two and three dimensional free-surface waves were studied. Different discretization orders and differentiation methods were considered, focusing on the linear distribution and finite difference schemes. The possible sources for numerical instabilities were addressed. A series of cases with and without forward speed was selected, and numerical investigations are presented. For the waves in three dimensions, the influence of the panels' aspect ratio and the waves' angle were considered. It has been shown that using the cancellation effects of different differentiation schemes the accuracy of the numerical method could be improved.

INTRODUCTION

Among the numerical methods applied for solving the wave-body interaction problem, Rankine panel method is one of the most popular. The flexibility provided by the simple Green function, makes this method applicable to a wide range of problems, from linear to non-linear, frequency-domain to time-domain. Moreover, its relative simplicity makes implementation cheaper, and easily expandable. Although, this method could not achieve the efficiency of the frequency-domain solvers, it is efficient enough for solving many practical hydrodynamic problems in comparisons to other alternatives such as volume methods. However, the advances in parallel computing makes the last statement subject to discussion and, in principle, case dependent.

Similar to any other numerical method, Rankine panel method introduces numerical inaccuracies into the ideal continuous solution. The importance of identifying and quantifying these inaccuracies has been known from the early applications of the method. These inaccuracies are particularly of importance when the propagation of waves on a discrete free-surface is of interest.

Longuet-Higgins and Cokelet were among the first to identify and report the presence of numerical instabilities in the Rankine source formulation. They adopted a mixed Eulerian-Lagrangian method for solving the wave propagation problem in [1] and identified the short-length numerical waves on top of the main solution, which had destabilization effects. Since the wave length of these instabilities were twice the size of the elements, they became to be known as saw-tooth instabilities.

In [2] Sclavounos and Nakos used Fourier analysis to study the dispersion and damping properties of the waves generated by a disturbance moving under the free surface with a constant velocity in two dimensions. They investigated the consistency and convergence of the discrete problem. The combination of finite difference schemes with constant panels were investigated in their paper. Moreover, they looked into the properties of a

continuous differentiation using a third order B-spline method (equivalent to a second order polynomial). They concluded that their method have better dispersion and damping properties than the constant element method. Moreover, they linked the numerical instabilities to the presence of spurious roots in the discrete dispersion relation. In [3] Romate also studied this problem independently by combining finite difference operators and higher order polynomials as shape functions.

Later on, Nakos extended the two-dimensional analysis to three dimensions in [4]. He studied the waves generated by a moving and harmonically oscillating disturbance under the free surface. He showed that the accuracy of the numerical method also depends on the elements' aspect ratio and $\tau = U\omega/g$. Moreover, he argued that the aliasing of the wave energy could be the reason behind the energy build-up in spurious roots and lead to the saw-tooth instability. Kim et al. in [5] used the numerical method from [4] and looked into the accuracy of the numerical method in capturing the waves traveling on the free surface in absence of current or forward speed. They investigated *temporal* stability and showed that it results in a Courant-type condition.

Raven in [6] considered the desingularization effects on the properties of a constant element method for the waves generated by a moving disturbance. Later in [7], Sierevogel studied the accuracy of both upstream and downstream waves using constant elements and finite difference methods in two dimensions. She also considered the time discretization schemes for numerical calculation of the time derivatives and investigated the temporal stability of her method. In [8] Bunnik, expanded the calculations in [7] to three dimensions. He also investigated the temporal stability using Z-transformation. He showed that, although central difference schemes have good dispersion and damping properties, they may lead to an unstable solution.

Büchmann in [9] studied the spatial and temporal convergence and stability of the B-spline method with shape-function differentiation. He also presented a Courant-type condition for stability, which depends on the discretization properties. Later in [10] he showed that the mentioned condition is not a *sufficient* but a *necessary* condition. He argued that forward speed (or current) could change the nature of the instabilities from saw-tooth, and reduce the frequency of the numerical waves. Recently, Kim et al. in [11] expanded the calculations for constant elements, with desingularization and collocation point shift, to include finite water depth effects as well.

In the present study the Fourier transformations of the continuous and discrete dispersion relations were utilized to investigate the relative accuracy of the combination of different finite-difference schemes and distribution orders in capturing the propagating two and three dimensional waves. The focus was on direct boundary integral formulation, i.e. source and dipole, and linear distribution. The present study is, in some areas, an extension to the previous studies mentioned above. Not all the aspects touched upon in the previous studies were covered here. In some parts, qualitative comparisons with previous findings are presented. The intention was to find out the limitation of different models and assess the influence of different types of discretization step by step. The analysis presented here is not complete. For instance, the influence of the grid non-uniformity and the forcing function were not taken into account and left for future works. As argued in [10], these may have influence on the properties of the numerical method.

FORMULATION

The direct boundary integral formulation, by distribution of Rankine sources and dipoles on the domain boundaries, was chosen to represent the solution for the velocity potential function (ϕ). The focus of attention here was on the error in estimating ϕ on the free surface. For this purpose, it was assumed that ϕ on the body was known. In other words, all the effects due to presence of the body were considered as a known forcing function. In this way, the direct boundary integral formulation could be rearranged as Eqn. (1) shown below.

$$C(\mathbf{x})\phi(\mathbf{x}) + \iint_{S_F} G(\mathbf{x},\xi)\frac{\partial\phi(\xi)}{\partial\mathbf{n}(\xi)}\,\mathrm{d}S - \iint_{S_F} \phi(\xi)\frac{\partial G(\mathbf{x},\xi)}{\partial\mathbf{n}(\xi)}\,\mathrm{d}S = F \tag{1}$$

Here, $\mathbf{n}$ is the normal vector to the boundary surface pointing inside the fluid domain, $G(\mathbf{x},\xi) = 1/|\mathbf{x}-\xi|$ is the Green function, S_F is the free surface, and C is the solid angle (see for instance [12]). Although the time parameter is omitted for clarity, ϕ is a function of both time and space ($\phi(\mathbf{x},t)$). F is the forcing function. The forcing function represents the integral of all the boundaries (S_R) except the free surface, as shown in Eqn. (2).

$$F(\mathbf{x},t) = \iint_{S_R} \phi(\xi)\frac{\partial G(\mathbf{x},\xi)}{\partial\mathbf{n}(\xi)}\,\mathrm{d}S - \iint_{S_R} G(\mathbf{x},\xi)\frac{\partial\phi(\xi)}{\partial\mathbf{n}(\xi)}\,\mathrm{d}S \tag{2}$$

Assuming the free surface to be flat and on the $z = 0$ plane by linearization, the third term in Eqn. (1) becomes zero. Moreover, the solid angle is equal to 2π on a flat free surface. The free surface was assumed to extend to infinity. A uniform current U in positive x direction, or alternatively a vessel with forward speed U in the negative x direction, was assumed. Linearizing the velocity potential about the mean incoming flow, the normal derivative of the velocity potential on the free surface could be substituted from the Neumann-Kelvin free surface boundary condition as shown in Eqn. (3),

$$2\pi\phi(\mathbf{x}) + \frac{1}{g}\iint_{S_F} \left[\phi_{tt}(\xi) + 2U\phi_{t\xi}(\xi) + U^2\phi_{\xi\xi}(\xi)\right] G(\mathbf{x},\xi)\,\mathrm{d}S = F \tag{3}$$

Taking a Fourier transform of Eqn. (3) with respect to x,y and t gives Eqn. (4). The convolution properties of the Green function, and Fourier transform of the derivatives were used in obtaining Eqn. (4) after separating the terms (more details could be found for instance in [2] and [11]).

$$2\pi\widetilde{\phi}+\left(\frac{(-\mathrm{i}\omega)^2}{g}+\frac{2U(-\mathrm{i}\omega)(\mathrm{i}k\cos\theta)}{g}+\frac{(\mathrm{i}k\cos\theta)^2}{g}\right)\widetilde{G}\widetilde{\phi}=\widetilde{F} \tag{4}$$

Here $\widetilde{\phi}$ is the continuous Fourier transform of the velocity potential and a function of (k,θ,ω) instead of (x,y,t). Using inverse Fourier transform, the velocity potential is obtained as,

$$\phi(x,y,t)=\frac{1}{8\pi^3}\int_0^{\infty}\int_{-\pi}^{\pi}\int_0^{\infty}\frac{\widetilde{F}}{\widetilde{\mathscr{W}}}e^{\mathrm{i}(\omega t-kx\cos\theta-ky\sin\theta)}k\,\mathrm{d}k\,\mathrm{d}\theta\,\mathrm{d}\omega \tag{5}$$

where

$$\widetilde{\mathscr{W}}=2\pi+\left(\frac{-\omega^2}{g}+\frac{2U\omega k\cos\theta}{g}+\frac{-k^2\cos^2\theta}{g}\right)\frac{2\pi}{|k|} \tag{6}$$

The poles of the integral's kernel ($\widetilde{\mathscr{W}}=0$) in Eqn. (5) correspond to the wave-like solutions of the velocity potential. Setting $\widetilde{\mathscr{W}}=0$ and rearranging the equation gives the familiar dispersion relation for a propagating wave (Eqn. (7)).

$$\widetilde{\mathscr{W}}=-\omega^2+2U\omega\cos(\theta)k-U^2\cos(\theta)^2k^2+g\,|k|=0 \tag{7}$$

Here the parameters of the Fourier transformation could be related to the physical properties of the waves. ω is the wave frequency, θ is the angle between x-axis and the wave propagation direction. $k=2\pi/\lambda$ is the wave number, where λ is the distance between two wave-peaks along the propagation axis. As expected, the representation of the problem using a continuous distribution of sources and dipoles, on a free surface extending to infinity, dose not change the dispersion relation. However, in other to solve the problem numerically, truncation and discretization of the free surface are needed. Truncation and discretization of the free surface introduce errors in the numerical model. These errors could be estimated by comparing the discretized version of the boundary integral formulation to the continuous form (see [2] and [3]). Here, the truncation effects were neglected and the focus was on discretization. Both space and time discretization could introduce errors and therefore are of importance. Since the errors in the free-surface's velocity potential were of interest, it was convenient to measure it in terms of the errors in the wave length (dispersion) and amplitude (damping or amplification).

Let us start by assuming the free surface to be discretized into infinite number of rectangular elements. The elements were assumed to be uniform in size with constant aspect ratio $\Lambda=\Delta y/\Delta x$, where Δx and Δy are the elements' spans in x and y directions, respectively. ϕ on the flat free surface could be represented using the B-spline base functions as shown in Eqn. (8).

$$\phi(\xi,\eta)=\sum_{j=1}^{N_V}\phi_j B_j^{(m)}(\xi,\eta) \tag{8}$$

Here N_V is the number of vertices on the surface, ϕ_j is the velocity potential weight at that vertex, and $B_j^{(m)}$ is a periodic, uniform, centered B-spline base function for a 2D surface with order m in parametric coordinates ξ and η, $B_j^{(m)}(\xi,\eta)=b^{(m)}(\xi)b^{(m)}(\eta)$. The one dimensional base functions are obtained from the recursive formula in Eqn. (9), where h is the panel span.

$$\begin{aligned} b^{(1)}(\xi)&=\begin{cases}1 & |\xi|\le\frac{h}{2}\\ 0 & \text{otherwise}\end{cases}\\ b^{(m)}(\xi)&=\frac{1}{h}\int_{-\infty}^{+\infty}b^{(m-1)}(\tau)b^{(0)}(\xi-\tau)\,\mathrm{d}\tau\end{aligned} \tag{9}$$

Using the discrete representation of the velocity potential in Eqn. (8), the integral over the free surface changes into a summation over the elements, which could be related to the summation over base functions. Although, this is directly applicable for the B-spline method, the constant panel method ([13]) and a uniform linear HOBEM ([14]) could also be related to these base functions by minor changes in the elements coordinate systems (see [15]). The properties of the B-spline method of order higher than two could be studied to give an indication of the numerical properties of HOBEM.

The B-spline base function is the same for all the elements. Therefore, different elements' base functions could be related to a single function at the origin by means of a simple translation (see for instance [2]). Using this property, the boundary integral formulation gets a discrete convolution form as shown in Eqn. (10).

$$\begin{aligned}&2\pi\sum_{j=-\infty}^{\infty}\phi_j B_{i-j}^{(m)}+\frac{1}{g}\sum_{j=-\infty}^{\infty}\left(\frac{\partial^2\phi}{\partial t^2}\right)_j\mathscr{S}_{i-j}\\&+\frac{2U}{g}\sum_{j=-\infty}^{\infty}\left(\frac{\partial^2\phi}{\partial x\partial t}\right)_j\mathscr{S}_{i-j}+\frac{U^2}{g}\sum_{j=-\infty}^{\infty}\left(\frac{\partial^2\phi}{\partial x^2}\right)_j\mathscr{S}_{i-j}=F\end{aligned} \tag{10}$$

Here, $B_{i-j}^{(m)}=B_0^{(m)}(\mathbf{x}_i-\mathbf{x}_j)$ and,

$$\mathscr{S}_{i-j}^{(m)}=\mathscr{S}_j^{(m)}(\mathbf{x}_i-\mathbf{x}_j)=\int_{-\infty}^{\infty}\int B_o^{(m)}(\xi)G(\mathbf{x}_i-\mathbf{x}_j-\xi)\,\mathrm{d}\xi\,\mathrm{d}\eta \tag{11}$$

where, $\mathbf{x}_i$ and $\mathbf{x}_j$ are the so-called field and source points, respectively. Getting semi-discrete Fourier transform of Eqn. (10)

and using the discrete convolution properties and aliasing theorem, the *discrete dispersion relation* is obtained, as shown in Eqn. (12) below, where $\widehat{(\,)}$ represents the semi-discrete Fourier transformation.

$$\widehat{\mathscr{W}} = 2\pi g + \widehat{D}^{(tt)} \frac{\widehat{\mathscr{S}}}{\widehat{B}^{(m)}} + 2U\widehat{D}^{(t)}\widehat{D}^{(x)} \frac{\widehat{\mathscr{S}}}{\widehat{B}^{(m)}} + U^2 \widehat{D}^{(xx)} \frac{\widehat{\mathscr{S}}}{\widehat{B}^{(m)}} = 0 \tag{12}$$

Here, $\widehat{D}$ is the semi-discrete Fourier transform of the differentiation operator, which depends on the method and the order of differentiation scheme (see for instance [16]). $\widehat{B}^{(m)}$ is the semi-discrete Fourier transform of the base function defined in Eqn. (13).

$$\widehat{B}^{(m)}(u,v) = \Delta x \Delta y \sum_{K,L=-\infty}^{\infty} \left(\frac{\sin \frac{u_K \Delta x}{2}}{\frac{u_K \Delta x}{2}} \right)^m \left(\frac{\sin \frac{v_L \Delta y}{2}}{\frac{v_L \Delta y}{2}} \right)^m \tag{13}$$

Here, u and v are the components of the wave number in x and y direction, respectively, and,

$$\begin{aligned} u_K &= u + \frac{2\pi K}{\Delta x} \\ v_L &= v + \frac{2\pi L}{\Delta y} \end{aligned} \tag{14}$$

where K and L are integer indexes for summation. $\widehat{\mathscr{S}}$ is the semi-discrete Fourier transform of Eqn. (11) shown in Eqn. (15).

$$\widehat{\mathscr{S}} = \sum_{K,L=-\infty}^{\infty} \widetilde{B}_o^{(m)}(u + \frac{2\pi K}{\Delta x}, v + \frac{2\pi L}{\Delta y})\ \widetilde{G}(u + \frac{2\pi K}{\Delta x}, v + \frac{2\pi L}{\Delta y}) \tag{15}$$

Here, $\widetilde{B}_o^{(m)}$ and $\widetilde{G}$ are continuous Fourier transforms of the base function and the Green function presented in Eqn. (16) and Eqn. (17), respectively.

$$\widetilde{B}^{(m)}(u,v) = \Delta x \Delta y \left(\frac{\sin \frac{u\Delta x}{2}}{\frac{u\Delta x}{2}} \right)^m \left(\frac{\sin \frac{v\Delta y}{2}}{\frac{v\Delta y}{2}} \right)^m \tag{16}$$

$$\widetilde{G} = \frac{2\pi}{\sqrt{u^2+v^2}} = \frac{2\pi}{|k|} \tag{17}$$

It is important to mention that if analytical differentiation is used to calculate the spatial derivatives, the differentiation operator will appear inside the summation of Eqn. (15).

Similar to the continuous problem, the roots of the discrete dispersion relation represent the wave-like solutions of the discrete problem. Ideally these roots in Eqn. (12) must be identical to the roots of the continuous dispersion relation in Eqn. (7). However, in reality this is not the case. Assuming a frequency ω, a current speed U, and an angle θ the possible wave number k is obtained by solving Eqn. (12). As mentioned before, the difference between the solution in the discrete and continuous problems could be evaluated in terms of the dispersion and damping errors. Following [7] and [8], the following relation between discrete (k_d) and continuous (k_c) wave numbers was assumed.

$$k_d = k_c(1 + C_r + \mathrm{i}C_i) \tag{18}$$

In this way, C_r is an indication to the dispersion error, while C_i represents the damping or amplification error. Looking at Eqn. (5), it is possible to conclude that $C_r > 0$ corresponds to shorter and $C_r < 0$ to longer numerical waves in comparison to the continuous waves, respectively. Moreover, $C_i < 0$ introduces damping, while $C_i > 0$ corresponds to amplification of the wave amplitude. It must be noted that the damping/amplification error due to discretization, i.e. C_i, must not be confused with an oscillating floating body damping coefficient due to generation of waves. Evaluations of the dispersion and damping errors for a series of different problems are presented in the following sections. If more than one root exist for the solution due to discretization, the results are shown only for the root closest to the continuous solution. In practice, filtering techniques must be used to remove the undesirable solution due to numerically appeared roots (see for instance [4]).

RESULTS AND DISCUSSIONS

Without forward-speed

To simplify the problem, the properties of the discrete dispersion relation were compared to the continuous one first by neglecting the forward speed. Moreover, it was assumed that the waves are traveling only in the positive x direction, which reduces the equations to two dimensions. Then, the continuous dispersion relation in Eqn. (7) reduces to Eqn. (19) below.

$$\widetilde{\mathscr{W}} = g|k| - \omega^2 = 0 \tag{19}$$

The discrete dispersion relation for this case could have different forms, depending on the continuous or discrete time and space assumptions.

Continuous time and discrete space: As a first step, a problem continuous in time and discrete in space was assumed. This is the case, for instance, when a steady harmonic wave problem on a discrete free surface is studied. The discrete dispersion relation for this problem is shown in Eqn. (20) below.

$$\widehat{\mathscr{W}} = 2\pi g \widehat{B}^{(m)} - \omega^2 \widehat{\mathscr{S}} = 0 \tag{20}$$

Here the time-derivative operator was substituted using a continuous Fourier transformation (see [15]). The obtained wave

numbers from the two dispersion relations, for different B-spline orders, are compared in Fig. 1 using the notation in Eqn. (18).

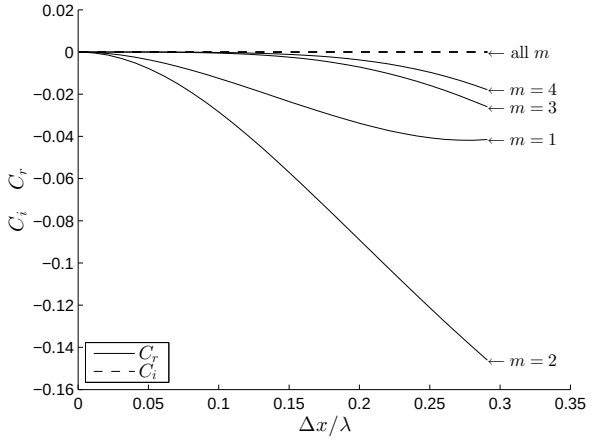

FIGURE 1. Dispersion and damping for waves without current, discretized space and continuous time, C_r: Dispersion, C_i: Damping, m: B-spline order, λ: Wave length., Δx: Element span in x

As Fig. 1 shows, discretized waves are longer than continuous waves. Meaning that the discretization introduces a *dispersion* error in the problem. As expected, the error approaches zero by reducing the element-span to wave length ratio. The error also depends on the order of discretization. It is interesting to point out that the linear elements ($m = 2$) give a more dispersive solution than constant panels ($m = 1$). This has been reported before also by [3] for linear polynomials. Increasing the order to more than $m = 2$ improves the dispersive properties significantly. The damping introduced due to the space discretization in this case is zero for all order of base functions. The dispersion error could be predicted, and controlled, by choosing a reasonable element-span to wave-length ratio for important waves in the problem.

Fig. 2 shows the relation between wave frequency and wave number from the discrete and continuous dispersion relations for different orders of space discretization. It is interesting to note that the wave group velocity (V_g), which is defined by the slope of $\omega - k$ curve, goes to zero when $\Delta x/\lambda$ approaches 0.5. As mentioned by [5], these waves correspond to the so-called saw-tooth waves, with a wave length $\lambda = 2\Delta x$. Since the group velocity approaches zero for these wave-lengths, they can not carry the energy away from the source. Therefore, the energy introduced by a disturbance, for instance an oscillating body, into these wave numbers accumulates in time. This could be one of the reasons behind the saw-tooth instability in the boundary integral solution of free surface waves, which was first mentioned by [1].

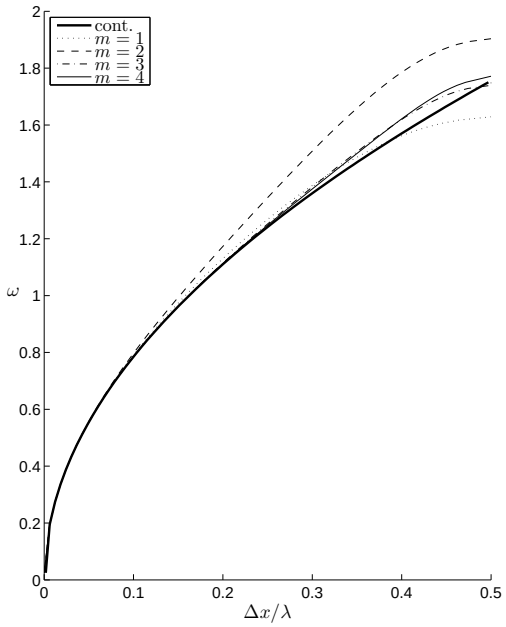

FIGURE 2. Frequency and wave number relation for discrete dispersion relation without current, discretized space and continuous time, ω: wave frequency, *Cont.*: Continuous solution, m: B-spline order, λ: Wave length, Δx: Element span in x

Discrete time and space: The combined time and space discretization was considered. The discrete dispersion relation, with both time and space discretization, and without current is shown in Eqn. (21) below.

$$\widehat{\mathscr{W}} = 2\pi g \widehat{B}^{(m)} + \widehat{D}^{(tt)} \widehat{\mathscr{S}} = 0 \tag{21}$$

The expression for $\widehat{B}^{(m)}$ and $\widehat{\mathscr{S}}$ could be found in Eqns. (13) and (15), respectively. $\widehat{D}^{(tt)}$ is the Fourier transform of the finite difference operator for the double derivative in time, which depends on the finite difference operator order.Here, a second order backward differentiation operator was chosen for double derivatives in time.

Fig. 3 shows the discrete wave dispersion and damping, with respect to $\Delta t/T$, for different values of B-spline order, and $\Delta x/\lambda$. As Fig. 3 suggests, for $\Delta x/\lambda = 0.05$ the accuracy of the numerical method is dictated by the time derivative scheme, and the B-spline order plays no significant role. As $\Delta x/\lambda$ increases to 0.12, the influence of the spatial discretization appears. By decreasing the time-step, the discrete problem converges to a solution which is different than the continuous solution. Moreover, increasing the B-spline order decreases the dispersion error. It is interesting to note that the damping factor C_i shows dependency to the spatial discretization order, although the introduced damping by the pure spatial discretization was zero in the time-continuous case (see Fig. 1).

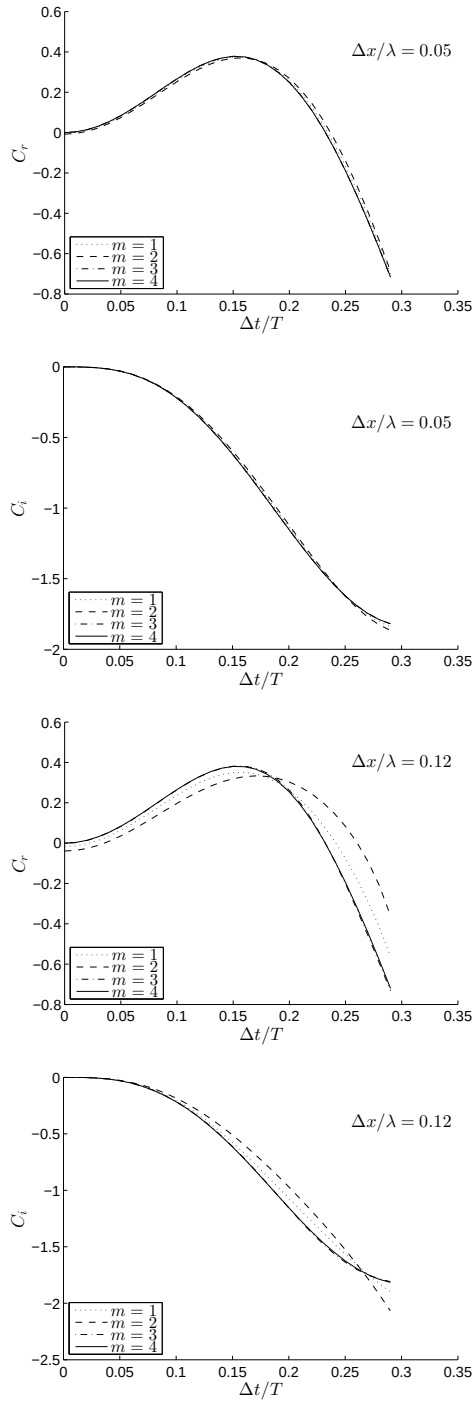

FIGURE 3. Dispersion and damping for waves without current, discretized time and space for different B-spline orders (m). C_r: Dispersion, C_i: Damping, m: B-spline order, λ: Wave length., Δx: Element span in x, T: Wave period, Δt: Time step

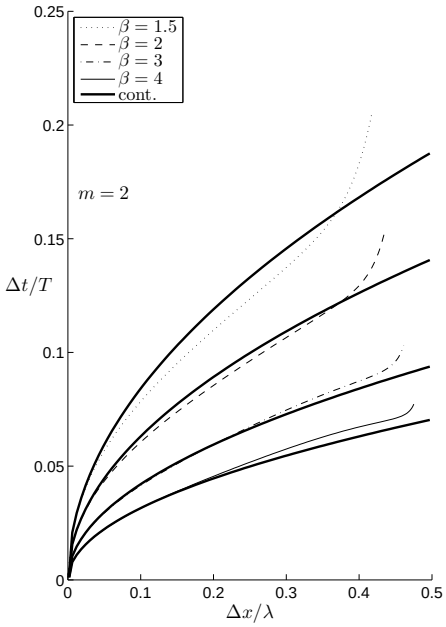

FIGURE 4. Frequency and wave number relation for discrete dispersion relation without current, discretized time and space, T: Wave period, Δt: Time step, *cont*.: Continuous solution, m: B-spline order, λ: Wave length., Δx: Element span in x, $\beta = \sqrt{\Delta x/(g\Delta t^2)}$

Fig. 4 compares the continuous and discrete dependency between the non-dimensional wave frequency and wave number, for linear spatial discretization. The second order backward difference operator was used for calculating the time double derivative. Different curves are plotted for different values of $\beta = \sqrt{\Delta x/(g\Delta t^2)}$, which indicates the relation between time-step and element-span. Comparing Fig. 4 with Fig. 2, it is possible to see that the group velocity no longer approaches zero for the saw-tooth wave number, and instead, it goes to infinity. This was true for all orders of spatial discretization. This effect may be related to the damping introduced by the time discretization. Therefore, presence of saw-tooth instabilities are less expected in this case. However, as it is mentioned in [10], making a general conclusion on the stability criteria for practical problems is not straight forward.

With steady forward speed

The steady wave pattern generated by a traveling disturbance, with velocity U in the negative x direction, and infinite water depth was considered. This is equivalent to the problem of a ship advancing with a steady forward speed in absence of waves. In this case, the generated waves travel at different angles with respect to the axis of forward motion (x). Then, the continuous dispersion relation in Eqn. (7) reduces to Eqn. (22)

below.

$$\widetilde{\mathscr{W}} = g\,|k| - U^2 k^2 \cos^2\theta = 0 \tag{22}$$

The discrete dispersion relation for the same problem is given in Eqn. (23), where $\widehat{D}^{(xx)}$ is the discrete Fourier transformation of the double derivative operator in x direction, and depends on the differentiation order. $\widehat{D}^{(xx)}$ is obtained using the discrete convolution properties of finite difference operators (see for instance [2] or [15]).

$$\widehat{\mathscr{W}} = 2\pi g \widehat{B}^{(m)} + U^2 \widehat{D}^{(xx)} \widehat{\mathscr{S}} = 0 \tag{23}$$

Considering three dimensional waves, the discrete dispersion relation in Eqn. (23) has two more parameters which influence the dispersion and damping properties of the numerical method. These are the wave propagation direction θ, and the elements' aspect ratio $\Lambda = \Delta y/\Delta x$. Focusing on the influence of the surface discretization by assuming a continuous differentiation operator ($\widehat{D}^{(xx)} = -k^2\cos^2(\theta)$) gives Eqn. (24).

$$\widehat{\mathscr{W}} = 2\pi g \widehat{B}^{(m)} - U^2 k^2 \cos^2(\theta) \widehat{\mathscr{S}} = 0 \tag{24}$$

Fig. 5 shows the dispersion error for different elements' aspect ratios and propagation directions of waves. Since the derivatives were assumed to be calculated analytically, the damping is zero for all the cases in Fig. 5. It is interesting to note that the dispersion error due to surface discretization is mostly positive. Meaning that the waves are shorter than they would be in a continuous solution. As expected, the error generally increases by increasing Λ or θ.

Different methods could be used for calculating the double derivative operator in x direction. Assuming a continuous and differentiable base function, the double derivative could be calculated analytically from the base function expression. In this case, the Fourier transform of the finite difference operator changes to the Fourier transform of a continuous differentiation. Moreover, a combination of a continuous and finite difference operators is also possible. Using the aliasing and the behavior of the integral kernel at infinity, the differentiation operator could be exchanged analytically between the base function and the source function (G). This is the case for the indirect boundary integral formulation, when one derivate is calculated using finite difference operator and the other by differentiating the source function (see for instance [13]). Sclavounos and Nakos studied, to some extend, different combinations of operators in [2] for their numerical method. For instance, they showed that the third order finite difference operator for calculating the double derivate in x direction leads to an unstable solution.

Here a second order finite difference operator was used for calculating the double derivatives in x direction. Fig. 6 shows the dispersion and damping properties for different propagation

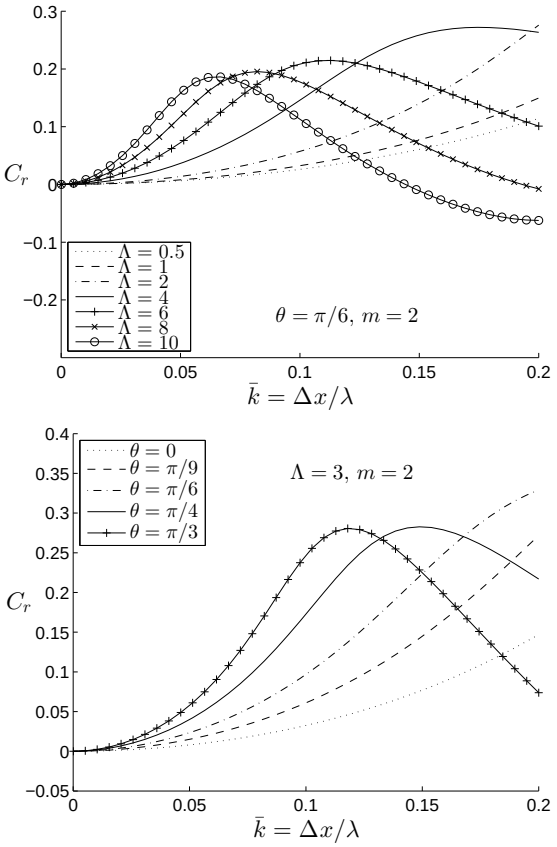

FIGURE 5. Dispersion and damping (steady forward speed) for surface discretization only, different wave propagation directions θ and element aspect ratio Λ. linear elements ($m = 2$), element aspect ratio $\Lambda = \Delta y/\Delta x$. C_r: Dispersion, θ: wave propagation direction. λ: Wave length.

directions. It is interesting to note that the dispersion errors have changed sign to negative (longer waves than continuous solution). This means that the chosen finite difference operator increases the resulted wave lengths numerically. As a consequence, the introduced dispersion error cancels the one from surface discretization. This cancellation is a function of the aspect ratio. Moreover, the waves propagating oblique to the current have better damping properties. This could be explained by considering the fact that the damping error is introduced by the double derivative operator in x direction. Therefore, the waves with smaller component in x-direction were less affected by the numerical differentiation.

With forward speed and oscillations

The complete form of the dispersion relation is of relevance for the waves generated by an oscillating disturbance with a constant forward speed. The full dispersion relation, assuming har-

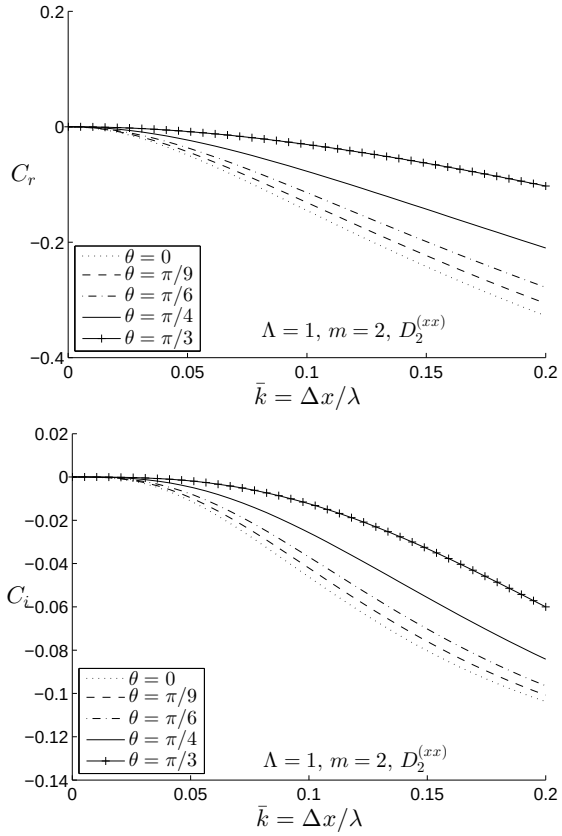

FIGURE 6. Dispersion and damping (steady forward speed) for different wave propagation directions θ. C_r: Dispersion, C_i: Damping,θ: wave propagation direction. λ: Wave length, $D_2^{(xx)}$: Second order finite difference operator for double derivative in x.

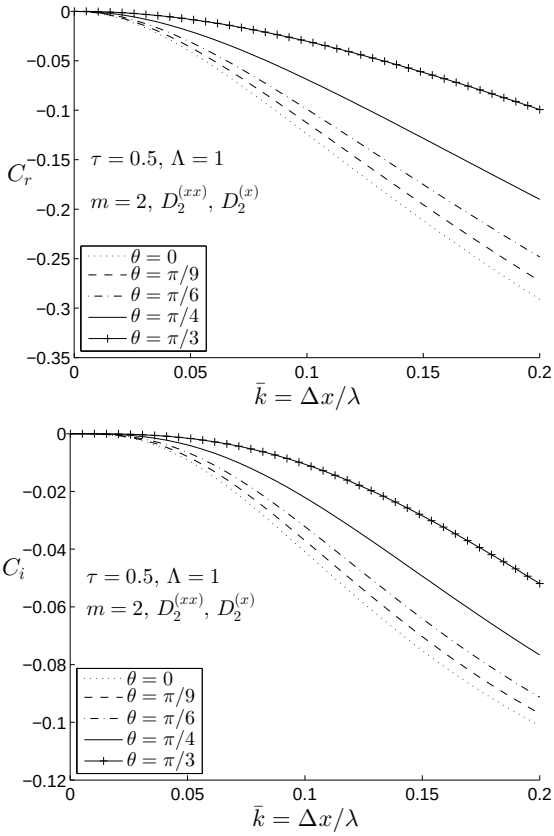

FIGURE 7. Wave dispersion and damping (forward speed and oscillations) on a discrete surface, continuous time, with a second order finite difference operator for the spatial derivatives. $\tau = U\omega/g$, θ: wave propagation direction, C_r: Dispersion factor, C_i: Damping factor, $\Lambda = \Delta y/\Delta x$: element aspect ratio.

monic steady-state oscillations, is presented in Eqn. (25). A study on the temporal stability of the problem could be found in [8] among others. The main focus here was on the performance of the numerical methods for capturing the steady harmonic solution of the problem.

$$\widetilde{\mathscr{W}} = g\,|k| - \omega^2 + 2U\omega k\cos(\theta) - U^2k^2\cos^2(\theta) = 0 \qquad (25)$$

Harmonic waves with discrete surface and spatial derivative: Harmonically oscillating waves on a linearly discretized surface with numerically calculated spatial derivatives, using second order finite difference operators, were assumed. Then, the discrete dispersion relation in Eqn. (12) reduces to Eqn. (26). The influence of different differential operators and discretization orders could be found in [4], [9] and [15] among others.

$$\widehat{\mathscr{W}} = 2\pi g\widehat{B}^{(m)} - \omega^2\widehat{\mathscr{S}} - 2\mathrm{i}U\omega\widehat{D}^{(x)}\widehat{\mathscr{S}} + U^2\widehat{D}^{(xx)}\widehat{\mathscr{S}} = 0 \quad (26)$$

Fig. 7 shows that the dispersion and damping of the downstream waves are governed by the finite difference operator used for differentiation in x-direction. As a consequence, the waves traveling oblique to the current have better properties. Similar behavior was discussed in steady forward speed case (see Fig. 6).

Fully discretized dispersion relation: The fully discretized dispersion relation in space and time was shown in Eqn. (12). The study was focused on linear elements (with B-spline base function of second order $m = 2$), together with second order finite difference operators for the spatial derivatives.

The first, second, and third order backward finite difference operators were used to calculate the single and double time derivatives. The coefficients for these operators could be found in [8] and [16] among others. Fig. 8 compares the dispersion and damping properties of different time derivative operators, with respect to the ratio between the time-step and the oscillations

period. The $\Delta x/\lambda$ ratio was chosen to be 0.01 in order to minimize the spatial error at this stage. The third order operator has the best dispersion properties. However, the positive C_i indicates amplification, which leads to an unstable scheme in time. The next best choice is the second order operator. This operator has a similar absolute dispersion error to the first order, however, has much better damping properties.

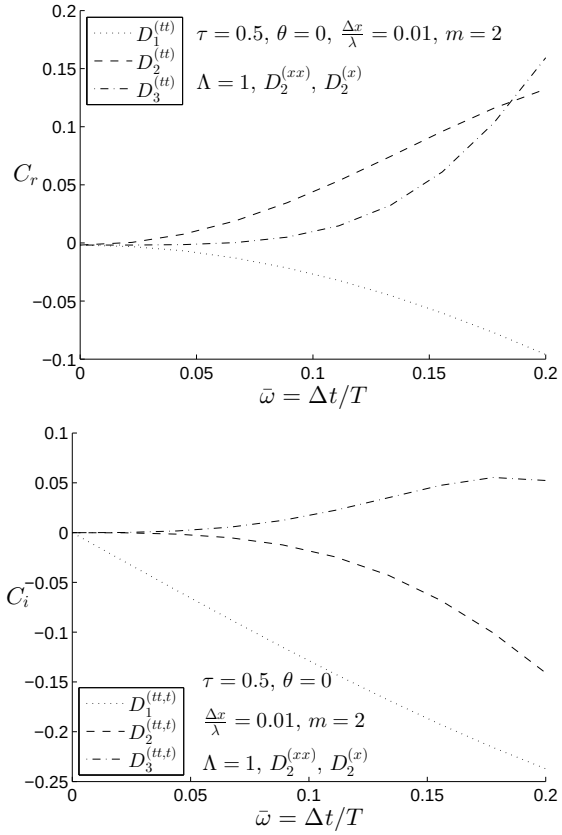

FIGURE 8. Downstream waves dispersion and damping (forward speed and oscillations) for different time discretization orders with a second order finite difference operator for the spatial derivatives. $\tau = U\omega/g$, θ: wave propagation direction, C_r: dispersion, C_i: damping, $\Lambda = \Delta y/\Delta x$: element aspect ratio.

Focusing on the second order backward difference for the time derivatives, Fig. 9 presents the dispersion and damping properties of different $\Delta x/\lambda$ ratios. The model's error approaches a non-zero value by reducing the time-step. The constant error, as expected, comes from the spatial discretization and the numerical calculation of derivatives, which reduces by reducing $\Delta x/\lambda$. By comparing the damping in Figures 8 and 9, one could expect that C_i, for the third order time marching method, becomes negative for small enough time-steps. In other words, the damping introduced by the spatial derivatives could stabilize the third order time marching scheme for small enough time steps.

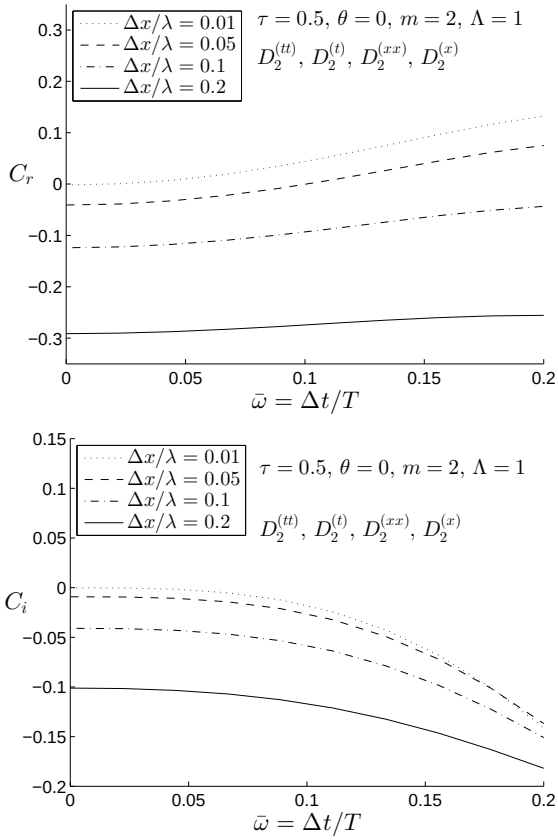

FIGURE 9. Downstream waves dispersion and damping (forward speed and oscillations) for different $\Delta x/\lambda$ ratio with second order finite difference operator for spatial and time derivatives. $\tau = U\omega/g$, θ: wave propagation direction, C_r: dispersion, C_i: damping, $\Lambda = \Delta y/\Delta x$: element aspect ratio.

CONCLUSIONS

The dispersion and damping errors introduced by discretization of space and time were investigated for Rankine panel method. The direct boundary integral formulation, i.e. distribution of sources and dipoles were considered. The presence of a body was neglected. The free surface was assumed to be flat and extended to infinity. The elements were assumed to be rectangular with uniform shape and arbitrary aspect ratios. The solution was assumed to be presentable using a summation of centered B-spline functions. Semi-discrete Fourier analysis was used to obtain the discrete dispersion relation in comparison to the continuous dispersion relation, following [2] and [8] among others. The influence of discretization of time and space on different levels were considered separately. The study were focused on the

linear distribution of unknowns and second order finite difference operators in time and space.

It was shown that, in absence of current/forward-speed the dispersion and damping properties were mostly governed by the time-discretization scheme. The influence of the space discretization only appeared for relatively fewer number of elements per wave length than regular practice. Assuming continuous time, unlike dispersion, the introduced damping was zero and independent of the space discretization order. By introducing discrete time, the damping became space discretization dependent. The waves' group velocity did not approach zero for saw-tooth wave length when both space and time discretization were considered.

The time-independent dispersion relation in presence of current/forward-speed was considered. Assuming continuous spatial derivative, the space discretization introduced positive dispersion error, i.e. the numerical waves became longer than the physical waves. The error was dependent on the direction of differentiation and panels' aspect ratios. Calculating the spatial derivative using a second order finite difference operator resulted in a negative dispersion error. Meaning, the error due to discrete differentiation canceled the error introduced by the space discretization to some extent.

The fully discretized dispersion relation was considered. The results for three different time derivative operators were presented. The relative importance of space and time discretization was touched upon. It was shown that it is possible to stabilize unstable time-marching methods using the damping introduced by the spacial derivatives.

ACKNOWLEDGMENT

This work was financially supported by the Research Council of Norway through the Centres of Excellence funding scheme AMOS, project number 223254 and CeSOS. While MARINTEK made the conference attendance and presentation possible.

REFERENCES

[1] Longuet-Higgins, M., and Cokelet, E., 1978. "The deformation of steep surface waves on water. II. growth of normal-mode instabilities". *Proceedings of the Royal Society of London, Series A (Mathematical and Physical Sciences),* ***364***(1716), pp. 1–28.

[2] Sclavounos, P. D., and Nakos, D., 1988. "Stability analysis of panel methods for Free-Surface flows with forward speed.". In Proceedings of the 17th symposium on Naval Hydrodynamics.

[3] Romate, J. E., 1989. "The numerical simulation of nonlinear gravity waves in three dimensions using a higher order panel method". PhD thesis, Universiteit Twente, Enschede, Netherlands, June.

[4] "Ship wave patterns and motions by a three dimentional rankine panel method". PhD thesis, Massachusetts Institute of Technology, USA.

[5] Kim, Y., Kring, D., and Sclavounos, P., 1997. "Linear and nonlinear interactions of surface waves with bodies by a three-dimensional rankine panel method". *Applied Ocean Research,* ***19***(5-6), pp. 235–249.

[6] Raven, H., 1996. "A solution method for the nonlinear ship wave resistance problem". PhD thesis, Delft University of Thechnology, June.

[7] Sierevogel, L., 1998. "Time-domain calculations of ship motions". PhD thesis, Delft University of Thechnology, Feb.

[8] Bunnik, T., 1999. "Seakeeping calculations for ships, taking into account the non-linear steady waves". PhD thesis, Delft University of Technology, Nov.

[9] Büchmann, B., 2000. "Accuracy and stability of a set of free-surface time-domain boundary element models based on b-splines". *International Journal for Numerical Methods in Fluids,* ***33***(1), May, pp. 125–55.

[10] Büchmann, B., 2001. "Theory and applications in stability of free-surface time-domain boundary element models". *International Journal for Numerical Methods in Fluids,* ***37***(3), pp. 321–339.

[11] Kim, Y., Yue, D. K., and Connell, B. S., 2005. "Numerical dispersion and damping on steady waves with forward speed". *Applied Ocean Research,* ***27***(2), May, pp. 107–125.

[12] Mantic, V., 1993. "A new formula for the c-matrix in the somigliana identity". *Journal of Elasticity,* ***33***(3), Dec., pp. 191–201.

[13] Dawson, C., 1977. "A practical computer method for solving ship wave problems". In Proceedings of the 2nd International Conference on Numerical Ship Hydromechanics, pp. 30–38.

[14] Liu, Y., Kim, C., and Lu, X., 1991. "Comparison of higher-order boundary element and constant panel methods for hydrodynamic loadings". *International Journal of Offshore and Polar Engineering,* ***1***(1), pp. 8–17.

[15] Ommani, B., 2013. "Potential-flow predictions of a semi-displacement vessel including applications to calm-water broaching". PhD thesis, Norwegian University of Science and Technology, Department of Marine Technology, Trondheim, Norway.

[16] Ommani, B., and Faltinsen, O. M., 2013. "Linear dynamic stability analysis of a surface piercing plate advancing at high forward speed". In Proceedings of 32 International Conference on Ocean, Offshore and Arctic Engineering (OMAE 2013).

[17] "Time domain ship motions by a three-dimensional rankine panel method". PhD thesis, Massachusetts Institute of Technology, USA.